Supporting Information
Temperature-Sensitive Growth Kinetics and Photoluminescence Properties of CdS Quantum Dots

Xiaogang Xue, Yang Huang, Zanyong Zhuang, Feng Huang and Zhang Lin*

State Key Laboratory of Structures, Fujian Institute of Research on the Structure of Matter,

Chinese Academy of Sciences, Fuzhou, Fujian 350002, China

* CORRESPONDING AUTHOR E-mail: zlin@fjirsm.ac.cn

Table of Contents

1. The UV-Vis absorption spectra of CdS QDs during growth at 100 and 66 ^{o}C

Figure S1 showed the typical evolution of the UV-Vis absorption spectra of CdS QDs during growth at 66 ^{o}C. The change of the average size *vs.* time could be obtained by calculating the size with the adsorption data.
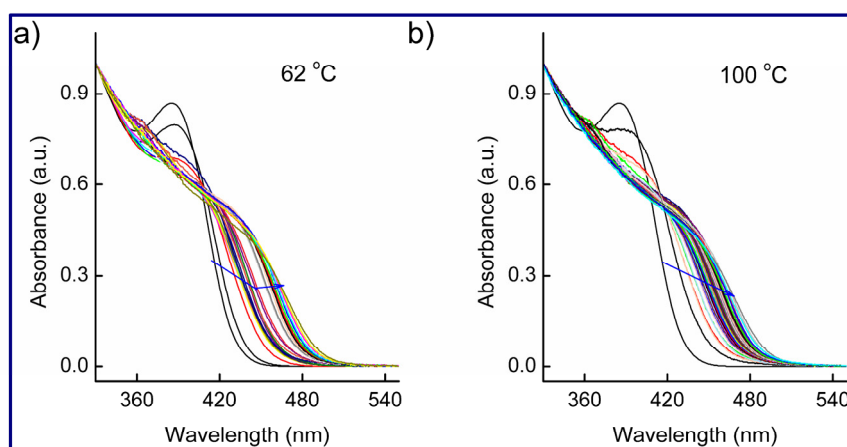

Figure S1. The temporal UV-Vis absorption spectra for CdS QDs during growth at 66 and 100 ^{o}C.

2. HRTEM images of CdS at representative time points during growth

Figure S2 shows typical HRTEM images of CdS QDs coarsened at 100 ^{o}C at representative time points in two steps.

Figure S3 shows typical HRTEM images of CdS QDs coarsened at 92 ^{o}C at representative time points in two steps.
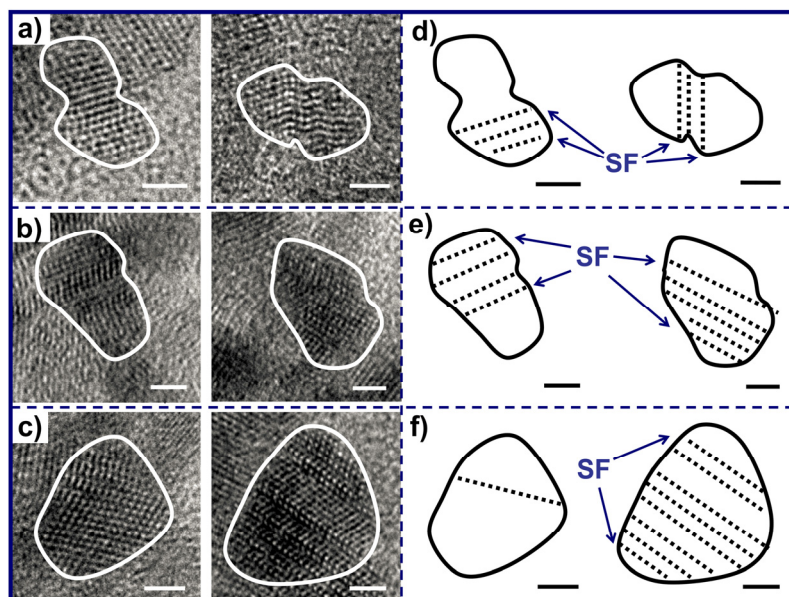
Figure S2. Typical HRTEM images of CdS QDs at CdS concentration coarsened at 100 °C at representative time points in a) step I' (10 min) and b-c) step II' (100 min, 400 min). Schematic outlines of each image illustrate the attachment scheme of OA. Scale bar is 2 nm.
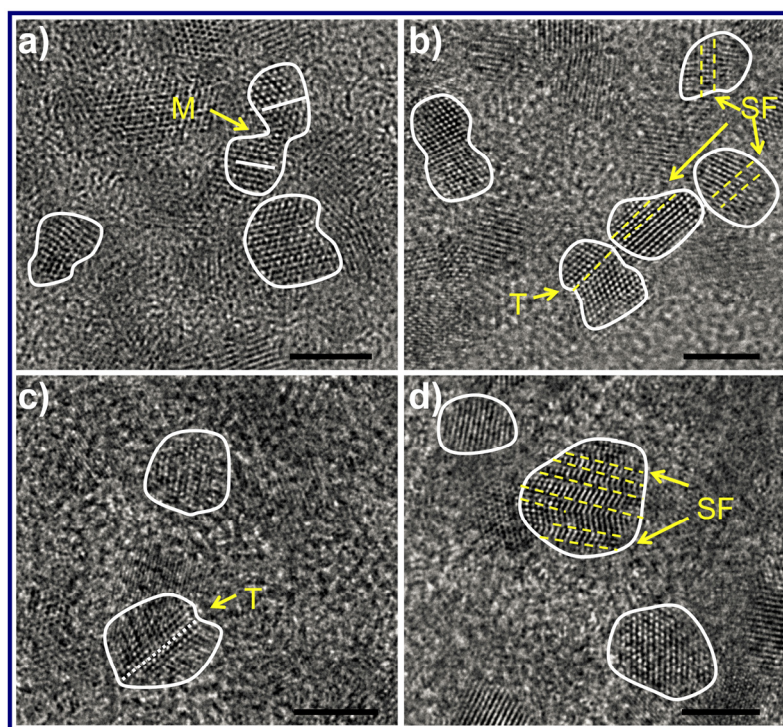

Figure S3. Typical HRTEM images of CdS QDs at CdS concentration coarsened at 92 °C at representative time points in step I' a) 10 min, b) 20 min and II' b) 200 min, c) 400 min. Schematic outlines of each image illustrate the attachment scheme of OA. Scale bar is 5 nm.

S3

3. The growth model for crystal growth at 100 $^{\circ}$C or 66 $^{\circ}$C

When fitting the experiment data of crystal growth by the solo "1+1" OA model[1] (blue dash line), as shown in Figure S4, fitting deviations for coarsening at 100 $^{\circ}$C is far larger than that at 66 $^{\circ}$C (as directed by arrows), suggesting different contributions of OR to crystal growth. Typically, the contribution of the OA is mainly from ~ 3.3 to 4.2 nm (0.9 nm), while the rest part of growth can be attributed to OR mechanism. It can be seen that the contribution of the OR growth at 100 $^{\circ}$C (Figure S4a) is about 0.8 nm, which is nearly equivalent to the contribution of the OA. While for coarsening at 66 $^{\circ}$C, the contribution of OR from step I to II is only about 0.2 nm, which is far smaller than that of the OA. Hence the growth from step I to II is dominated by the OA.
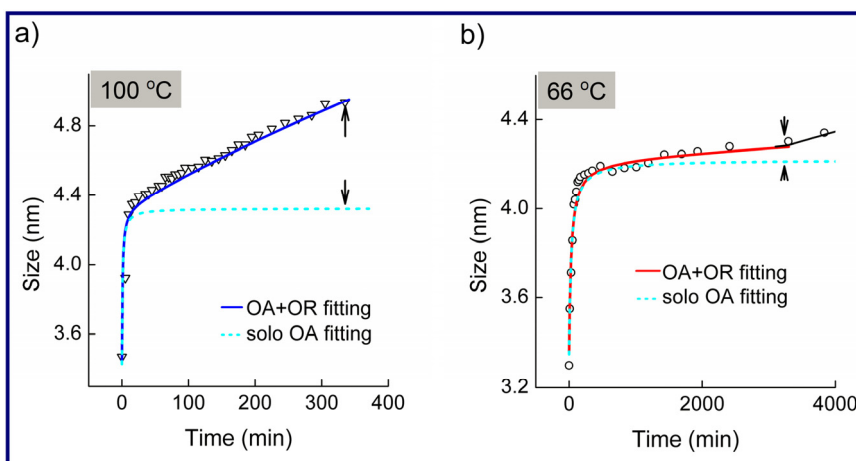

Figure S4. Experimental data (scatter), OA+OR fitting (solid line) and OA fitting (dash line) of the size of QDs as function of growth time for CdS QDs at 100 and 66 $^{\circ}$C.

Table 1. Estimated Values of Kinetic Parameters by Fitting the Experimental Data with OA+OR model (equ 2. in main text).

T ($^{\circ}$C)	n_1	k_{OA} (1/min)	k_{OR1} (nm^n/min)
66	2.0	0.031	0.00017
74	2.1	0.0886	0.0007
82	2.1	0.1886	0.0022
92	3	0.5	0.035
100	3	1.1	0.12

4. Quantitative FTIR analysis to detect the amount of thiol on the surface of particles

In order to detect the amount of surface adsorbed thiol, quantitative Fourier Transform Infrared Spectroscopy (FTIR) analysis was conducted. In detail, potassium Thiocyanate (KSCN, peaked near 2100 cm^{-1}) taken as the internal standard was firstly mixed with KBr. CdS sample with certain quantitative amount was blended with above powder. After that, press powder into a pellet for measurement. Figure S5 shows the FTIR spectra of TGA-capped CdS and KSCN mixture. In the spectra, no S–H absorption peak at 2550 cm^{-1} of thioglycolic acid (HOOCCH$_2$SH) was observed, indicating that the ligand is bound to the CdS particles through the thiolate functional group. Hence, the absorption bands of C=O (1626 cm^{-1}–1562 cm^{-1}) can be used for the quantitative analysis. Accordingly, as shown in Table S2, the relative content of HOOCCH$_2$SH vs. time at 66 and 100 ^{o}C in the TGA-capped CdS QDs growth system can be worked out.

Table S2. The relative content of HOOCCH$_2$SH on the CdS QDs surface vs. time in 66 and 100 ^{o}C growth system

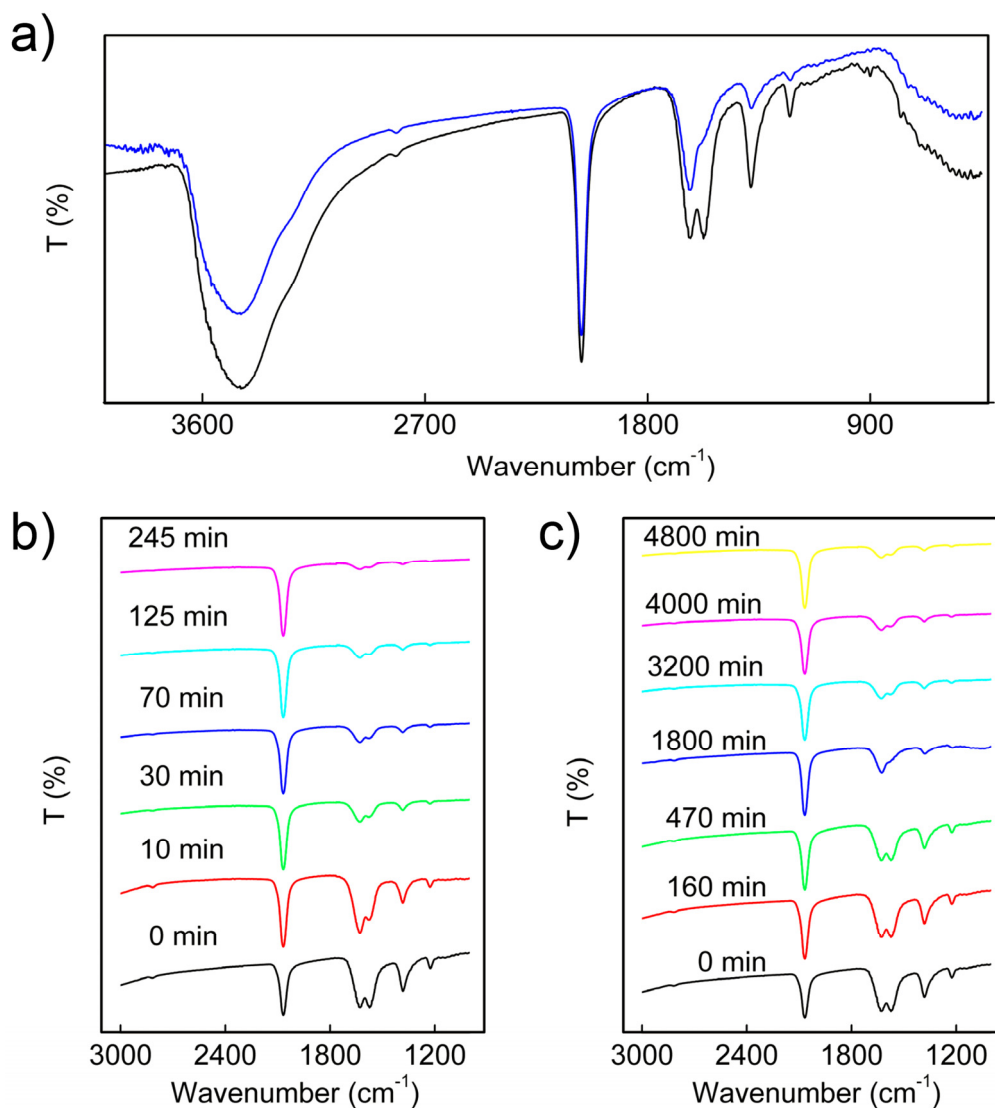| 66 ^{o}C		100 ^{o}C	
Time (min)	Content (%)	Time (min)	Content (%)
0	100	0	100
160	66	10	64
470	44	30	34
1800	40	70	22
3200	33	125	14
4000	20	245	5
4800	12		

Figure S5. FTIR spectra of the mixture of mercaptoacetic acid capped CdS taking KSCN as an internal standard. a) The TGA-capped CdS QDs at transition point of from step I to II (black line) and from I' to II' (blue line), b) The CdS particles hydrothermally treated at 100 °C, c) The CdS particles hydrothermally treated at 66 °C for different growing time.

5. Gaussian deconvoluted and normalized PL spectra of TGA-capped CdS

QDs at representative time point of growth at 100 °C

The defect-related PL emission centered at ~ 620 nm (D1) was decreased during the period from the latter step I' to II', with continuous red shift of its peak position toward 650 nm. The band-edge emission peaked at ~ 460 nm (E) emerged and the defect-related PL emission centered at ~ 725 nm (D2) were enhanced, but with almost constant peak positions.(Figure S6a). Gaussian deconvolution of the PL spectra (Figure 6b-d) confirms the split defect-related emission band, and shows the evolution tendency of D1 and D2, which was ascribed to the adjustment of the twin faults by previously reports. [2]
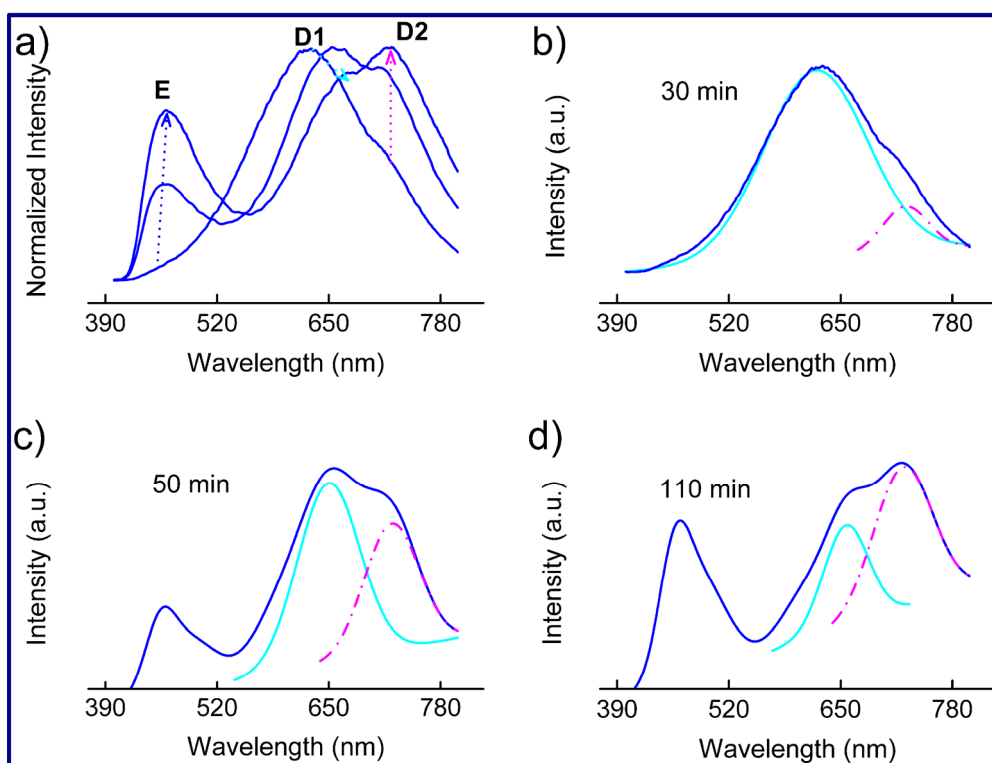

Figure S6. (a) The normalized PL spectra of TGA-capped CdS QDs at representative time point of step I' and II' (30, 50, 110 min) at 100 °C, (b-d) Gaussian deconvolution of the PL spectra of of TGA-capped CdS QDs at 30, 50, 110 min.

Reference

1. F. Huang, H. Z. Zhang and J. F. Banfield, *Nano Lett*, 2003, **3**, 373-378.
2. T. Y. Zhai, X. S. Fang, Y. S. Bando, Q. Liao, X. J. Xu, H. B. Zeng, Y. Ma, J. N. Yao and D. Golberg, *Acs Nano*, 2009, **3**, 949-959.